SUPPLEMENTAL FIGURES

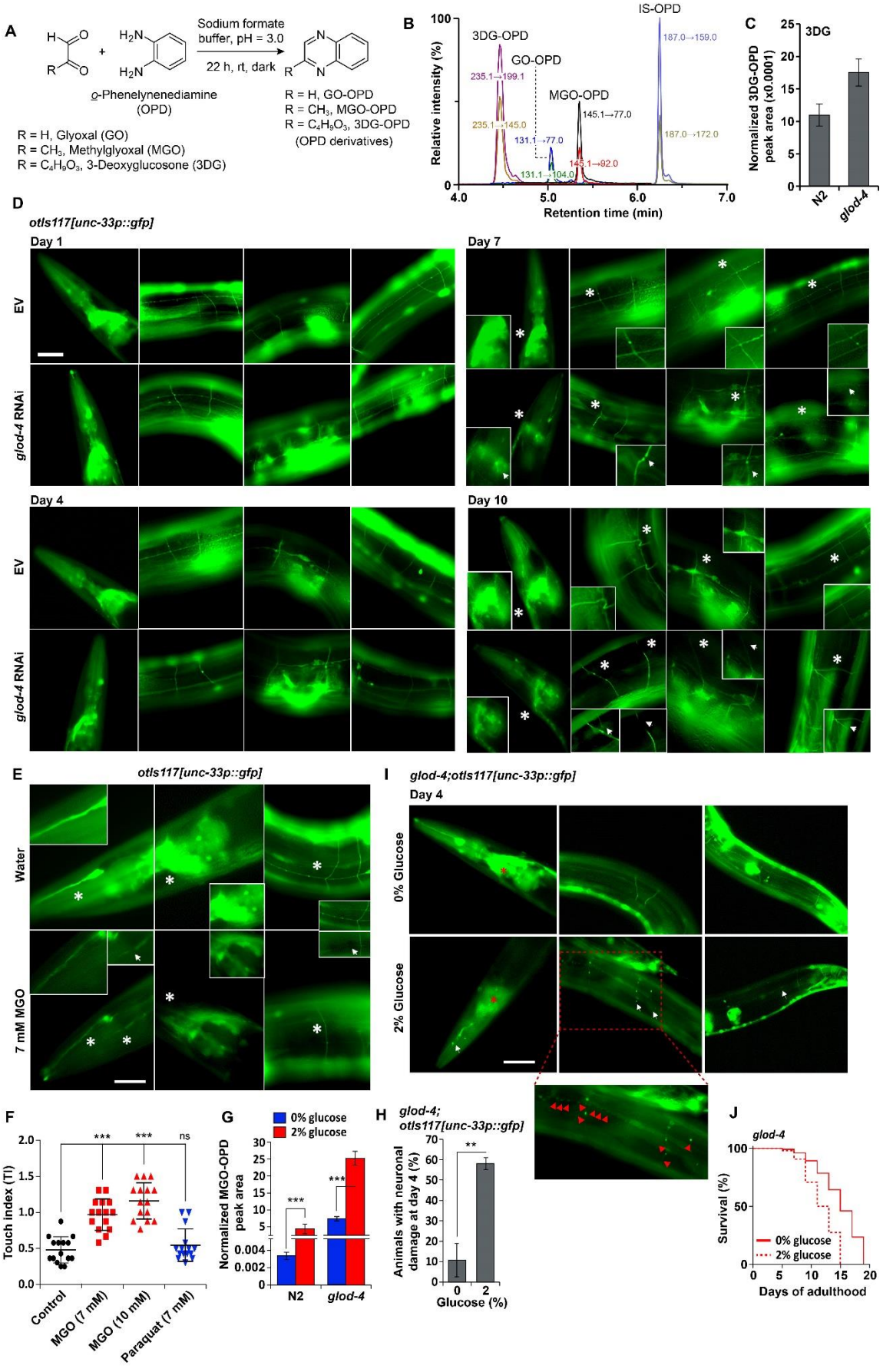

Figure S1. LC-MS/MS-based estimation of α-DCs and Neuronal damage due to *glod-4* knockdown. Related to Figure 1.

(A) Reaction conditions for derivatization of α-DCs with *o*-phenylenediamine (OPD).
(B) Extracted ion chromatograms (EICs) for MRM transitions, characteristic of OPD derivatives for synthetic 3DG, GO, and MGO (each compound injected at 5 pmol). 2,3-Hexanedione is used as internal standard (IS).
(C) Levels of 3DG in N2 and *glod-4* animals.
(D) Fluorescence microscopy images of *unc-33p::gfp* (pan-neuronal GFP) reared on empty vector (EV, L4440) or *glod-4* RNAi at days 1, 4, 7, and 10 of adulthood. Arrows and asterisk mark areas for comparison between EV and *glod-4* RNAi fed animals. Damages in the neuronal processes are classified as thinning or break in dendrites, abnormal axon/dendrite branching, or reduced fluorescence in the nerve ring. Scale bar 50 µm.
(E) Fluorescence microscopy images of *unc-33p::gfp* (pan-neuronal GFP) supplemented with water (control) or 7 mM MGO. Arrows and asterisk mark areas for comparison between control and 7 mM MGO-treated animals. Damages in the neuronal processes are classified as thinning or break in dendrites, abnormal axon/dendrite branching or reduced fluorescence in the nerve ring. Scale bar 50 µm.
(F) Touch index (TI) during young adult stage (~L4 + 8-10 h) for N2 animals, supplemented with water (control), 7 mM MGO, 10 mM MGO, or 7 mM Paraquat.
(G) Levels of MGO in *glod-4*, reared on media supplemented with 0 or 2% glucose.
(H) Neuronal damage in *glod-4;unc-33p::gfp* (pan-neuronal GFP) on day 4 of adulthood, reared on media supplemented with 0 or 2% glucose. n = 45.
(I) Fluorescence microscopy images of *glod-4;otls117[unc-33p::gfp]* (pan-neuronal GFP) reared on media supplemented with 0 or 2% glucose at day 4 of adulthood. Arrows point to damages in the neuronal processes in 2% glucose-treated animals, either as thinning/break in dendrites, abnormal axon/dendrite branching, or reduced fluorescence in the nerve ring. Red asterisk marks reduced fluorescence in the nerve ring of glucose-treated animals compared to control. Scale bar 50 µm.
(J) Survival curves for *glod-4* animals reared on media supplemented with 0 or 2% glucose.

Data are represented as mean ± SD. Significance: **P*<0.05, ***P*<0.005 and ****P*<0.0005.

See Table S2 for lifespan data.

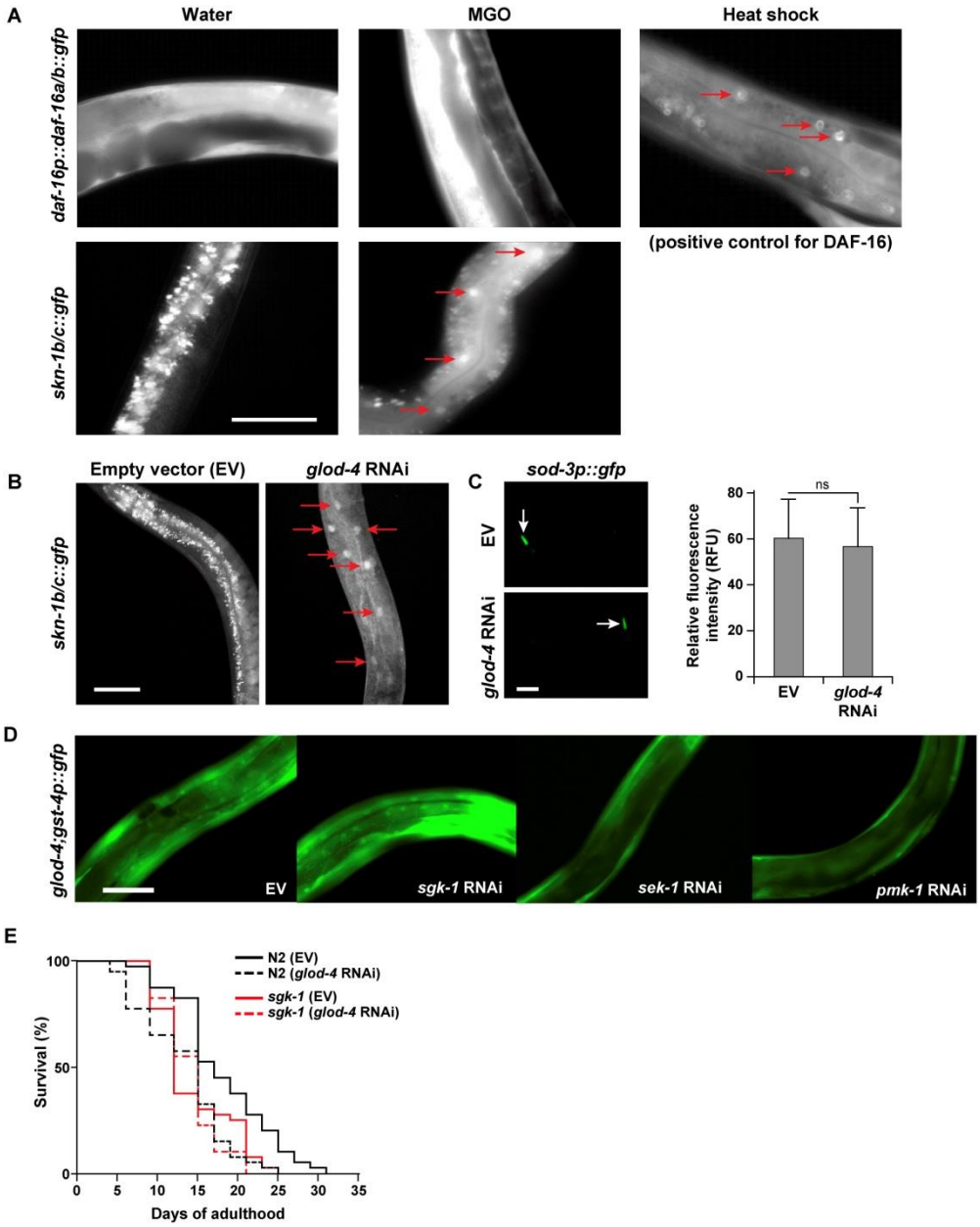

Figure S2. SKN-1 activation due to exogenous MGO treatment and specificity of downstream response to α-DC stress. Related to Figure 2.

(A) Fluorescence microscopy images depicting nuclear localization of DAF-16::GFP and SKN-1::GFP supplemented with water (control) or 7 mM MGO. Heat shock was used as a positive control to drive DAF-16 nuclear localization. Red arrows point towards nuclear localized transcription factors (SKN-1 and DAF-16). Scale bar 50 µm.
(B) Fluorescence microscopy images depicting nuclear localization of SKN-1::GFP reared on empty vector (EV, L4440) or *glod-4* RNAi. Red arrows point towards nuclear localized transcription factors of SKN-1. Scale bar 50 µm.
(C) (Left) Fluorescence microscopy images and (Right) quantification of relative fluorescence intensities of *sod-3p::gfp* animals (expression primarily on the pharynx region, indicated with a white arrow), reared on EV or *glod-4* RNAi. Scale bar 0.15 mm.
(D) Fluorescence microscopy images to observe GFP foci in *glod-4;gst-4p::gfp* animals reared on EV, *sgk-1*, *sek-1*, or *pmk-1* RNAi. Scale bar 50 µm.
(E) Survival curves for N2 and *sgk-1* mutant animals reared on EV or *glod-4* RNAi.

Data are represented as mean ± SD. Significance: **P*<0.05, ***P*<0.005 and ****P*<0.0005.

See Table S2 for lifespan data.

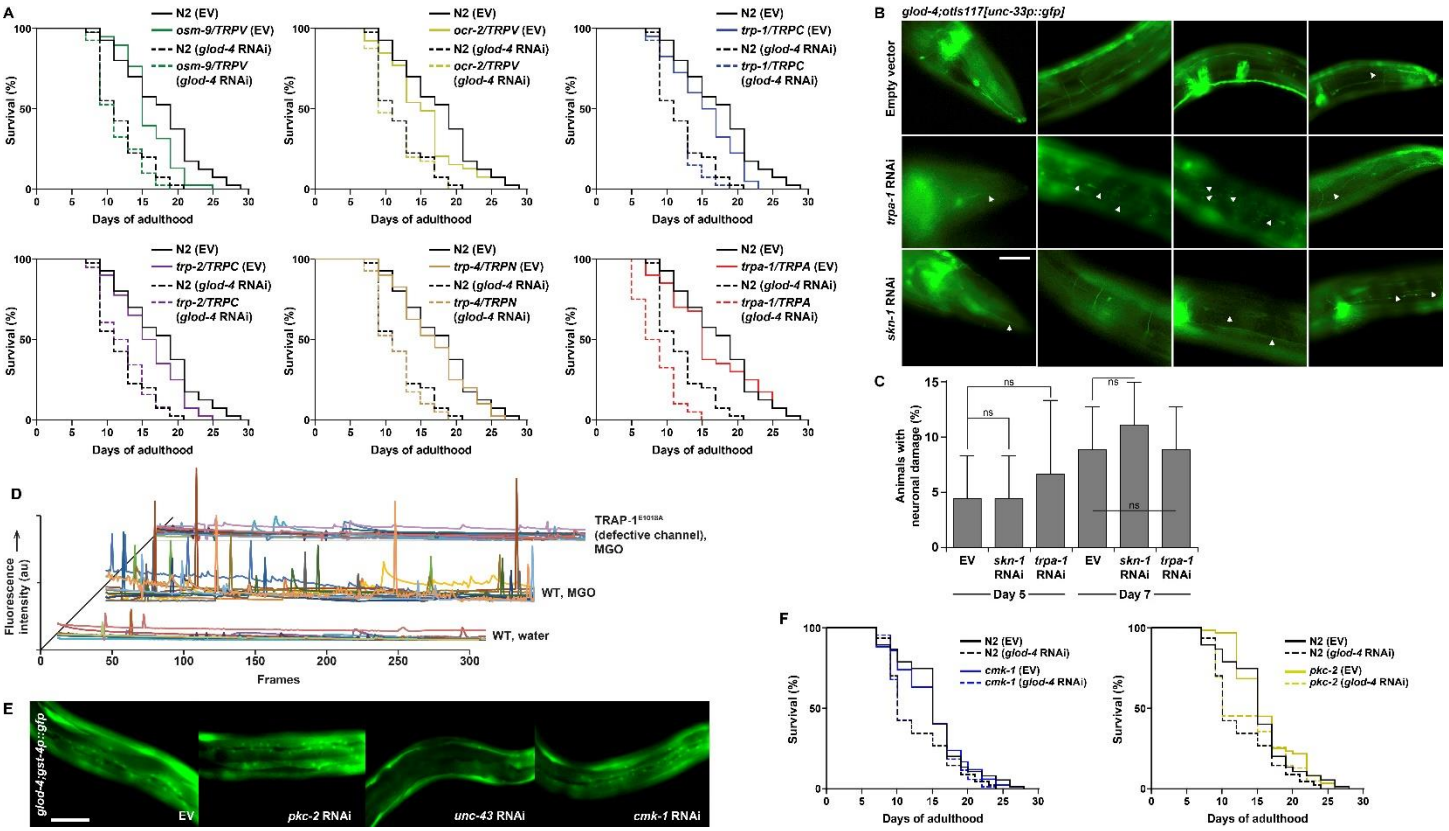

Figure S3. TRPA-1 is a sensor for α-DCs and result in SKN-1 activation. Related to Figure 3.

(A) Survival curves for N2 and various *C. elegans* TRP channel mutants animals reared on empty vector (EV, L4440) or *glod-4* RNAi.
(B) Fluorescence microscopy images of *glod-4;unc-33p::gfp* (pan-neuronal GFP) reared on EV, *trpa-1*, or *skn-1* RNAi during day 5 of adulthood. Red arrows point to damages due to *trpa-1* or *skn-1* knockdown in the neuronal processes: discontinuity in dendrites, breaks in commissures, thinning of neuronal processes, along the length of the body from head to tail at multiple areas. Scale bar 50 µm.
(C) Neuronal damage in *unc-33p::gfp* (pan-neuronal GFP) at days 5 and 7 of adulthood reared on EV, *skn-1*, or *trpa-1* RNAi. n = 45
(D) Fluorescence intensity traces for transgenic animals expressing an intestinal GCaMP1.3 (Ca^{2+} sensor) containing a wild-type TRPA-1 (WT) or TRPA-1^{E1018A} (Ca^{2+}-impermeable) channel mutant in response to 7 mM MGO or water. Each colored line indicates the trace for a single animal.
(E) Fluorescence microscopy images to observe GFP foci in *glod-4;gst-4p::gfp* animals reared on EV, *pkc-2*, *unc-43*, or *cmk-1* RNAi. Scale bar 50 µm.
(F) Survival curves for N2, *cmk-1*, and *pkc-2* animals reared on EV or *glod-4* RNAi.

Data are represented as mean ± SD. Significance: **P*<0.05, ***P*<0.005 and ****P*<0.0005.

See Table S2 for lifespan data.

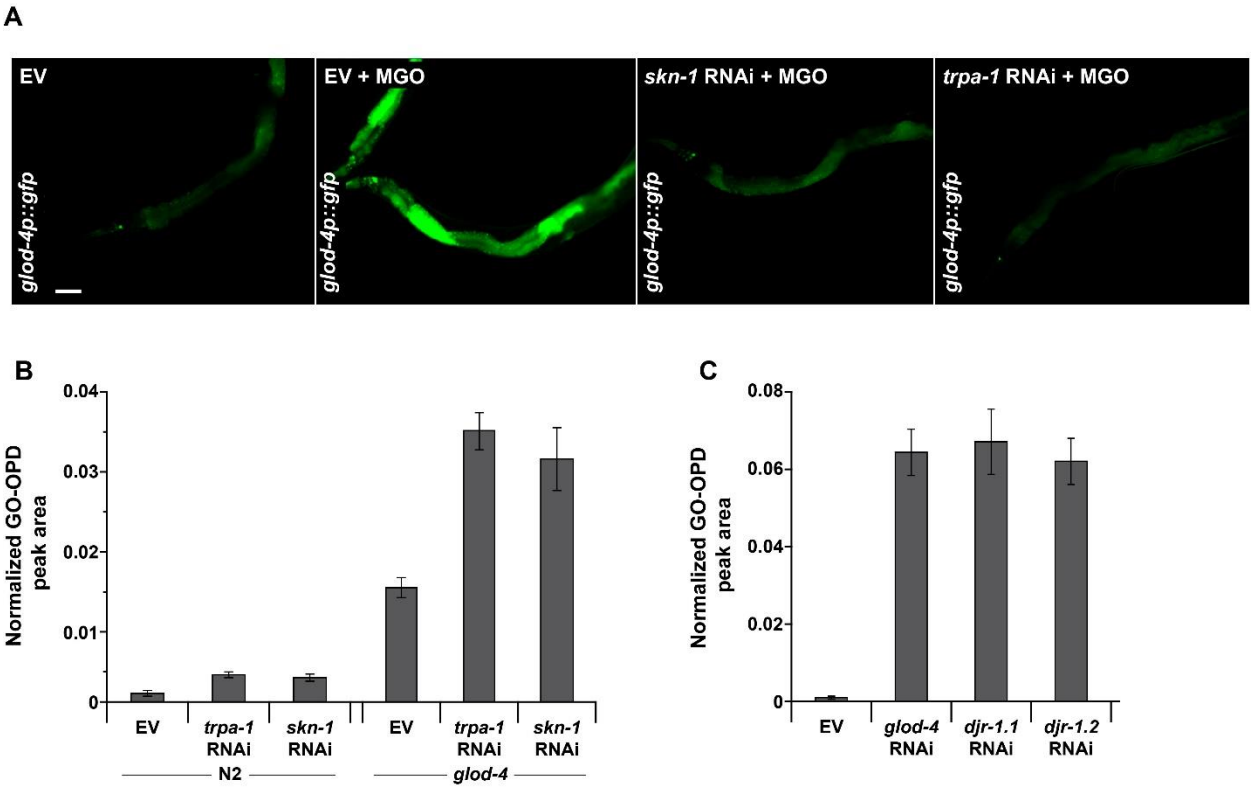

Figure S4. Downstream glyoxalases mediate α-DC detoxification in response to TRPA-1/SKN-1 activation. Related to Figure 4.

(A) Fluorescence microscopy representing GLOD-4 expression in *glod-4p::gfp* animals reared on empty vector (EV, L4440), *skn-1*, or *trpa-1* RNAi, supplemented with water (control) or 7 mM MGO. Scale bar 70 μm.
(B) Levels of GO in N2 and *glod-4* animals. Animals were reared on EV, *trpa-1*, *or skn-1* RNAi.
(C) Levels of GO in N2 reared on EV, *glod-4*, *djr-1.1*, or *djr-1.2* RNAi.

Data are represented as mean ± SD.

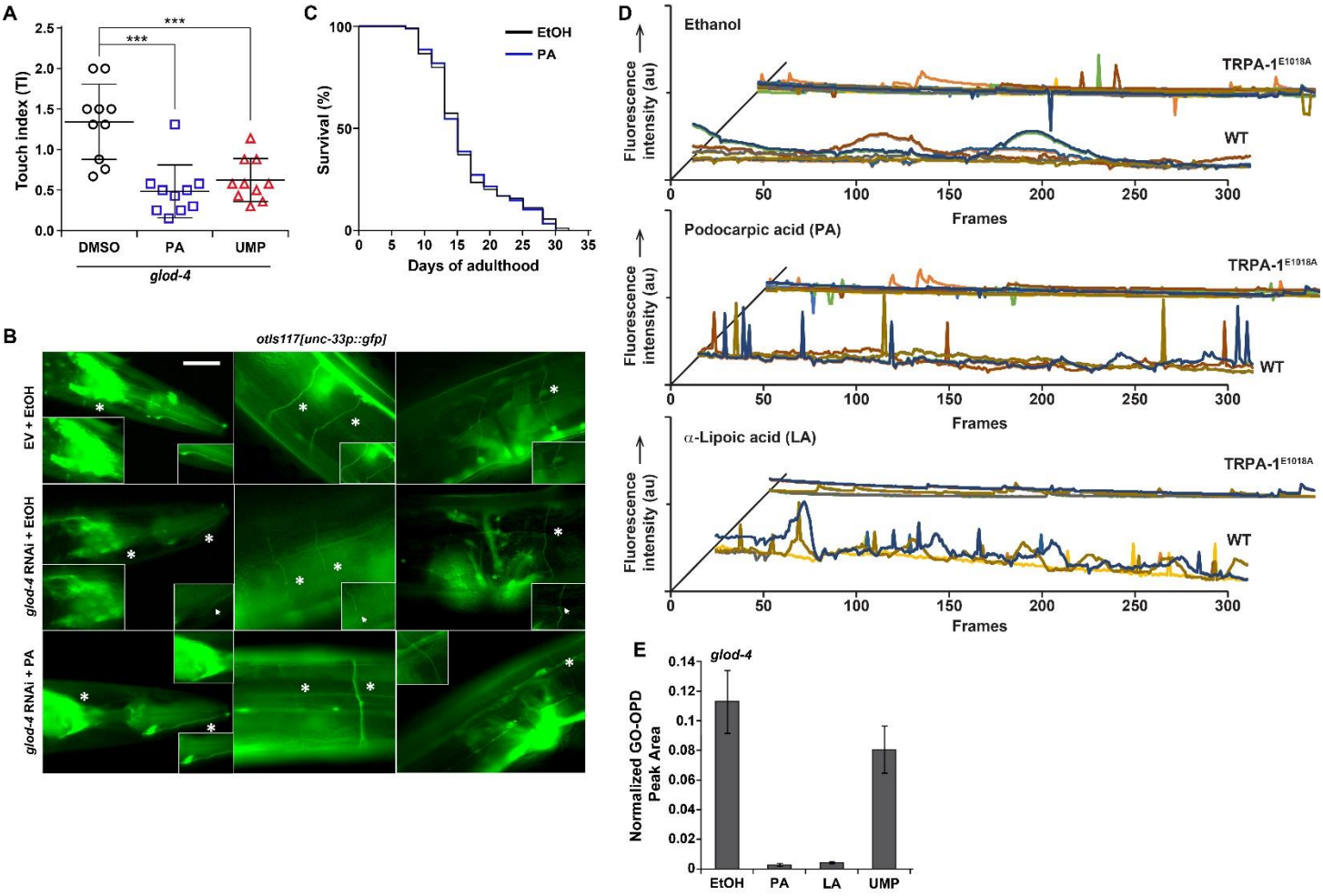

Figure S5. Podocarpic acid (PA) and α-Lioic acid (LA) rescues *glod-4* phenotypes and TRPA1 activation by allyl isothiocyanate (AITC) or MGO. Related to Figure 5.

(A) Touch indices (performed as part of a drug screen of TimTec NPL640) during young adult stage for *glod-4*, supplemented with DMSO (control), PA, or UMP (66.7 µM in DMSO).
(B) Fluorescence microscopy images of *unc-33p::gfp* (pan-neuronal GFP) animals at day 10 supplemented with EtOH (control) or PA (50 µM), reared on empty vector (EV, L4440) or *glod-4* RNAi. Asterisks indicate regions of interest that have been magnified. Arrows point to damages in the neuronal processes in animals reared on *glod-4* RNAi treated with EtOH (no drug), either as dendritic breaks, thinning of neuronal processes or reduced fluorescence in the nerve ring.
(C) Survival curves for N2 animals supplemented with EtOH (control) or PA (20 µM), reared on OP50-1.
(D) Fluorescence intensity traces in transgenic animals expressing an intestinal Ca^{2+} sensor GCaMP1.3 containing a wild-type TRPA-1 channel (WT) or a Ca^{2+} impermeable channel mutant (TRPA-1^{E1018A}) in response to ethanol (control), or 20 µM of PA or LA. Each colored line indicates the trace for a single animal.
(E) Levels of GO in N2 and *glod-4* animals treated with EtOH (control), PA, LA, or UMP (20 µM each).

Data are represented as mean ± SD. Significance: **P*<0.05, ***P*<0.005 and ****P*<0.0005.

See Table S2 for lifespan data.

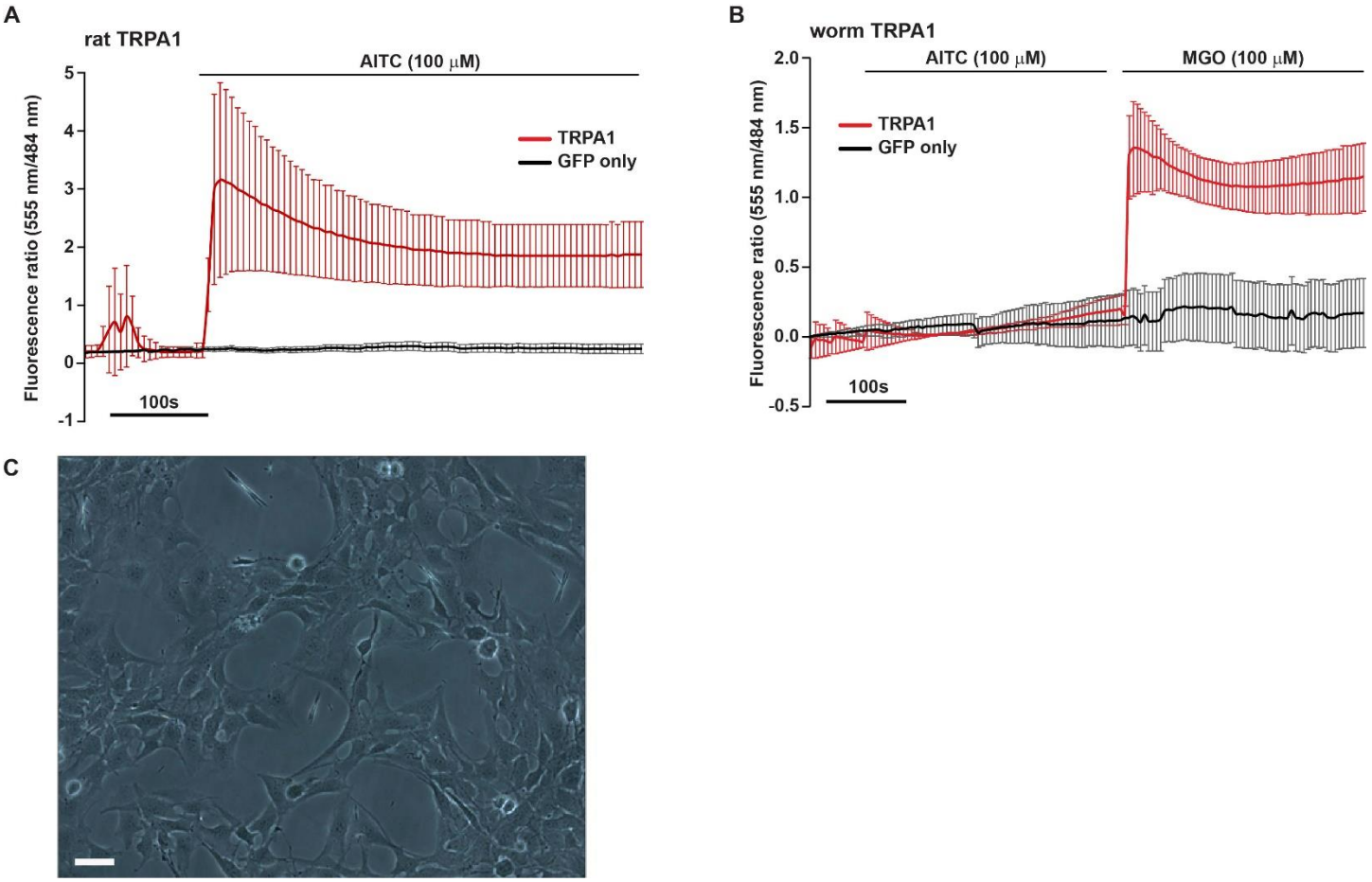

Figure S6. Podocarpic acid (PA) and α-Lioic acid (LA) rescues *glod-4* phenotypes and TRPA1 activation by allyl isothiocyanate (AITC) or MGO. Related to Figure 6.

Fluorescence ratio (555/484 nm) changes for the membrane-permeable Ca^{+2} indicator Rhod-3 AM in HEK293 cells transfected with
(A) TRPA1 (rat) and GFP or GFP only. Cells were treated with 100 µM allyl isothiocyanate (AITC).
(B) TRPA1 (worm) and GFP or GFP only. Cells were treated with 100 µM AITC first and then switched to 100 µM MGO.
(C) Bright-field microscopy image of 50B11 cell line (12 h post differentiation) showing neuron-like characteristics. Scale bar 50 µM.

Data are represented as mean ± SD.

SUPPLEMENTAL TABLE

Table S1: LC-MS/MS parameters for various α-DC-OPD derivatives. Related to Figure 1.

Analyte	MRM Precursor Q_1 (*m/z*)	MRM Product Q_3 (*m/z*)	Nature of MRM Transition $Q_1 \rightarrow Q_3$ (*m/z*)	Declustering potential, DP (V)	Entrance potential, EP (V)	Collision energy, CE (V)	Collision exit potential, CXP (V)	Retention time, RT (min)
Glyoxal-OPD (GO-OPD)	131.1	77.0	Quantifier	90	5.2	41.0	5.7	5.4 ± 0.07
		104.0	Qualifier	80	9.8	30.0	7.3	
Methylglyoxal-OPD (MGO-OPD)	145.1	77.0	Quantifier	65	8.1	40.0	12.0	5.1 ± 0.04
		92.0	Qualifier	65	10.2	30.0	5.5	
3-Deoxyglucosone-OPD (3DG-OPD)	235.1	199.0	Quantifier	74	8.0	23.0	12.0	4.5 ± 0.06
		145.0	Qualifier	74	8.0	31.0	9.0	
2,3-Hexanedione-OPD (IS-OPD)	187.0	159.1	Quantifier	60	5.1	31.0	12.3	6.3 ± 0.09
		172.0	Qualifier	50	10.8	27.0	16.5	

SUPPLEMENTAL EXPERIMENTAL PROCEDURES

Growth and maintenance

Worms were cultured at 20 °C for at least two generations under standard growth conditions on 5X *Escherichia coli* OP50-1 bacterial strain (cultured overnight at 20 °C at 220 rpm) before using for respective experiments [S1] and allowed to grow overnight. For feeding RNAi bacteria, synchronized L1 larvae were transferred to NGM plates containing 1 mM of isopropyl β-D-1-thiogalactopyranoside/IPTG (referred to as RNAi plates) seeded with 20X concentrated HT1115 bacteria (cultured overnight at 20 °C at 220 rpm), carrying desired plasmid for RNAi of a specific gene or bacteria carrying empty vector pL4440 as control and allowed to grow on plates for 48 h. For drug assays, synchronized L4 larvae were transferred to either 60 mm NGM plates (with or without IPTG), freshly seeded with 5X *E. coli* OP50-1 or 20X HT1115 RNAi bacteria. Before seeding, the desired drug (or vehicle control) was mixed with the bacteria. Final drug concentrations were calculated considering the total volume of media and bacteria seeded on the NGM plates.

Note: For *glod-4* animals, we found that the pathogenic phenotypes discussed in this paper are contingent on strictly maintaining an *ad lib* feeding regimen. Hence, care was taken to not to allow the animals to starve by maintaining a low worm to bacteria ratio and transferring to fresh plates frequently (at least once every two days).

Lifespan assay

Life span assays were performed in Thermo Scientific Precision incubators at 20 °C. After alkaline hypochlorite treatment, synchronized L1 animals were either placed onto NGM plates seeded with 5X concentrated *E. coli* OP50-1 (cultured on Lysogeny Broth/LB overnight) or on RNAi plates supplemented with 20X HT1115 RNAi bacteria. Post-L4 stage of development, all lifespan assays were performed using FUdR (5-fluoro-2 deoxyuridine) plates to inhibit development and growth of progeny. Every two to three days, animals were transferred on to new 60 mm NGM or RNAi plates freshly seeded with OP50-1 or HT1115 bacteria (with or without drug), respectively. 40-120 animals were considered for each lifespan experiment. Animal viability was assessed visually or with gentle prodding on the head. Animals were censored in the event of internal hatching of the larvae, body rupture, or crawling of larvae from the plates.

Assay for assessing neuronal damage

Neuronal damage was assayed using a pan-neuronal GFP reporter strain under different conditions and at different days of adulthood. Animals were paralyzed using freshly prepared 5 mM levamisole in M9 buffer and mounted on 2% agar pads under glass coverslips. Neuronal damage was visually inspected under an upright Olympus BX51 compound microscope coupled with a Hamatsu Ocra ER digital camera. Images were acquired under 40X objective. Neuronal deterioration was examined and characterized by loss of fluorescent intensity of nerve ring, abnormal branching of axon/dendrite, and thinning and fragmentation of axons and neuronal commissures. Quantification and imaging of animals harboring damage was performed using the Image J™ software (http://imagej.nih.gov/ij/). To reduce experimental bias, this assay was performed genotype-blind.

SKN-1 activation assay

Adult animals were examined for SKN-1 activation using GFP reporters for both SKN-1 and SKN-1 target genes: *gst-4* and *gcs-1*. For exogenous MGO and drug assays, age-synchronized GFP reporter strains were subject to control and treatment conditions for a period of 4-6 hours before microscopy. For RNAi-induced activation studies, GFP reporter strains were fed on HT1115 bacteria expressing empty vector pL4440 or RNAi gene from L1 stage. Synchronized day 1 adult animals were then subjected to microscopic examination. Activation of SKN-1 using SKN-1 fusion reporter was determined as described earlier [S2, S3]. Scoring for downstream SKN-1 targets carrying GFP reporter for *gcs-1* promoter was performed based on a previous study[S4] and categorized as follows: 'high' for strong GFP signal throughout the intestine, 'medium' for GFP signal in the anterior or posterior section of the intestine and 'low' for weak or no signal. For animals with *gst-4* promoters carrying GFP reporters number of GST-4 positive foci was counted under different conditions as described previously [S5]. Quantification of acquired images was done using the Image J™ software (http://imagej.nih.gov/ij/).

glod-4p::gfp expression assay

Transgenic adult animals carrying *glod-4p::gfp* were assayed. Fluorescent intensity was calculated by background subtraction and quantified for the same region of interest across individual animals. All quantification was done using Image J™ software (http://imagej.nih.gov/ij/).

Swim-bend assay for health-span assessment

Motility is a determinant of healthspan and rhythmic behavioral patterns as observed in *C. elegans* crawling versus swimming are direct functions of neuromuscular activity [S6]. *C. elegans* lateral swimming movements was measured as previously described as 'thrashing' [S6, S7] by scoring number of body bends per 30 seconds in S-medium. This gave a direct measure of the swim bend frequency and hence a relative measure of healthspan of the animal under different conditions.

Analytical instrumentation and software

High performance liquid chromatography (HPLC) was performed using a Shimadzu UFLC prominence system fitted with following modules: CBM-20A (Communication bus module), DGU-A_3 (degasser), two LC-20AD (liquid chromatograph, binary pump), SIL-20AC HT (auto sampler) and connected to a Phenomenex's Kinetex® EVO C18 column (2.1 x 150 mm, 5 µm, 100 Å). Mass spectrometry (MS) was performed using a 4000 QTRAP® LC-MS/MS mass spectrometer from AB SCIEX fitted with a Turbo V™ ion source. AB SCiex's Analyst® v1.6.1 was used for all forms of data acquisition, development of HPLC method, and optimization of analyte-specific MRM (multiple reaction monitoring) transitions. AB SCiex's Piekview® v2.1 and Skyline® v3.5 [S8] was used for LC-MS/MS data analysis.

Preparation of metabolome extracts and synthetic standards

Worms were cultured on NGM agar plates as explained before for lifespan experiments with some modifications: ~100 animals/60 mm plates were used for each experimental replicate and animals were harvested at day 4 of adulthood with 20 µL M9 buffer in 1.5 mL eppendorf tubes. Worm suspensions were flash-frozen over liquid nitrogen and subsequently homogenized ultrasonically using a Fisher Scientific's 550 Sonic Dismembrator with 80 µL of sodium formate buffer (pH = 3) containing 75 µM of 2,3-hexanedione (internal standard, IS). Two 20 s pulses at amplitude setting 4 of the instrument (on ice) were sufficient to completely homogenize worm bodies. To each homogenate tube 20 µL of 100 mg/mL *o*-phenelynediamine (OPD) solution in sodium formate buffer (pH = 3) were added, and the mixture was allowed to react in dark at room temperature for ~22 h. The long reaction time and the pH are critical parameters in this protocol: first to ensure complete derivatization of α-DCs bound reversibly to protein/glutathione –SHs; and second to prevent *in vitro* α-DC generation from glycolytic intermediates (DHAP, GAP, etc.) or due to DNA breakdown [S9]. At the end of the stipulated reaction window, 12 µL of 5 M perchloric acid was added to each tube and incubated on ice for 30 min to ensure complete protein precipitation. Subsequently, the tubes were centrifuged at 10,000 rpm for 10 min, and the supernatant collected and neutralized with 30 µL 4 M NH_4OH solution. All *glod-4*-derived samples (except with podocarpic acid or α-lipoic acid treated animals) were diluted 50-fold with methanol and 1 µL of each sample injected for LC-MS/MS analysis; all other samples were injected (1 µL) without dilution.

Synthetic standards for glyoxal, methylglyoxal, and 3-deoxyglucosone were obtained from Sigma-Aldrich, St. Louis, MO. Corresponding OPD derivatives were prepared as mentioned before (with IS), starting with 20 µL solution of each of these compounds in M9 at the following concentrations: 5 mM, 500 µM, 50 µM, and 5 µM. As previously noted [S10], almost quantitative derivatization was achieved after ~12 h of reaction for synthetic standards. Each of these samples were diluted 50-fold with methanol at the end to achieve individual 100 µM, 10 µM, 1 µM, and 100 nM solutions, 1 µL of which were injected for LC-MS/MS analysis. For every batch of worm samples analysis, a set of synthetic standards were processed.

Note: Recent reports [S11, S12] suggest the use of 0.3% sodium azide to the OPD derivatization mix to prevent acid-stable peroxidases from generating MGO and GO from OPD and resulting in α-DC over-estimation. For *glod-4*, such peroxidase-catalyzed OPD breakdown was found to be insignificant, i.e. azide addition had no detectable difference and was thus not used for this method.

MRM optimization, LC-MS/MS conditions, and data analyses

Optimization of analyte-specific MRM transitions, such as determination of suitable precursor and product ions and optimal MS parameters for each transition (Q_1, precursor → Q_3, product) were achieved by isocratic flow injection of the 10 µM solution (final) for each standard- or IS-OPD derivatives. The most intense (Q_1→ Q_3) transition was used as quantifier, whereas the next best transition was used as qualifier for each compound (Table S1). For LC separation, a solvent gradient of 0.1% acetic acid in water (aqueous) - methanol (organic) was used with 0.4 mL/min flow rate, starting with an acetonitrile content of 3% for 0.7 min, which was increased to 100% over 6 min and held at 100% for 1.5 min. The LC column was subsequently reconstituted to its initial condition (methanol content of 3%) over the next 0.5 min and re-equilibrated for 3 min.

Derivatized metabolome extracts, as well as synthetic α-DCs were analyzed by scheduled LC-MRM in positive ion mode. To develop the scheduled LC-MRM method, MS/MS data was collected for all transitions across the length of each LC run for a mixture of synthetic GO-, MGO-, 3DG-, and 2,3-hexanedione (IS)-OPD derivatives (1 µL injection of 1 µM final concentration). Source conditions were as follows: curtain gas (CUR) 20, nebulizer gas (GS1) 60, auxiliary gas (GS2) 50, ionspray voltage (IS) 4500 V, and source temperature (TEM) 450 ˚C. This step was undertaken to ascertain the LC retention times (RT) for the OPD derivatives. Several such sets were acquired to compute analyte-specific variability in RTs. Next, the MS was switched to operate in scheduled MRM mode, whereby the mass spectrometer acquired data for specific MRM transitions ±45 s around the computed RT for the analyte (Table S1). Relative quantification of GO, MGO, and 3DG were based on intetegration of corresponding OPD derivative-specific quantifier peaks obtained from scheduled LC-MRM runs (peak areas) and adjusted to the number of animals. To account for OPD derivatization efficiencies in individual tubes, sample-to-sample variability in MS response, and differential sample dilutions (both for synthetic α-DCs as well as α-DCs in worm homogenates), the peak areas were normalized to the quantifier peak area for IS-OPD for each sample.

Ca^{+2} flux-based channel studies in *C. elegans*

Ca^{2+} flux was measured using an upright Olympus compound microscope (BX51) under a 40X objective. Real time sequential G-CaMP1.3 fluorescent images were captured using Hamamatsu Ocra-ER digital CCD camera at a frame rate of 10 frames per second and for a span of 300 frames. Acquired images were analyzed for further intensity measurements using HC Image software v. 1.1.3.0 (Hamamatsu Corp., NJ). Percentage change in fluorescent peak intensity was estimated using the intensity values generated real time by the program.

Reverse transcription polymerase chain reaction (RT-PCR)

Total RNA was extracted from nearly 100 age-synchronized adult animals picked and collected in 20 µl of M9 buffer using TRIzol reagent (Life Technologies, CA). Subsequently, 1 µg total RNA was used as template for cDNA synthesis. cDNA was synthesized using the iScript™ cDNA synthesis kit (Bio-Rad, CA) following manufacturer's protocol. qRT-PCR was carried out using the SensiFAST SYBR No-ROX kit (Bioline, MA) in a LightCycler 480 Real-Time PCR system (Roche Diagnostics Corp., IN). Quantification was performed using the comparative $\Delta\Delta C_t$ method and normalization for internal reference was done using actin gene *act-1*. All assays were performed with 3 biological replicates using synchronized animals of age day 1 adulthood.

High-throughput drug screen in *C. elegans*

Synchronized *glod-4* L1 animals were cultured on NGM agar plates seeded with *E. coli* OP50-1 until L4. Animals were then transferred into individual wells (10 animals per well) of 96-well plates for high-throughput screening (NPL640, TimTec LLC, DE); each well containing 150 µL of 66.7 µM of individual drug (1 µL of 10 mM drug stock in DMSO) in S-medium. Post-transfer into wells, animals were fed OP50-1 bacteria *ad libitum* while incubating at 20 °C on a rocker for 12 h. DMSO was used as control. Post-incubation with drug or DMSO, animals were transferred from wells onto NGM agar plates seeded with OP50-1 bacteria. Touch assay was performed on individual animal and touch index (TI) was calculated for each compound from the library as mentioned earlier. Compounds that showed an amelioration of the hypersensitivity phenotype of *glod-4* young adult animals in this screen were subjected to a secondary screen for amelioration of the short lifespan phenotype associated with *glod-4* animals.

Growth, maintenance, drug administration, and imaging of 50B11 cell line

50B11 cells (immortalized rat DRG neuronal cells) maintain self-replication capability over many cell divisions (>300). The results described in this article were obtained with cells between 100 and 400 passages. Cells were grown in antibiotic treated complete Neurobasal media containing glucose, L-glutamine, Fetal Bovine Serum (FBS), B-27 supplement, and nerve growth factor (NGF) (100 ng/ml). Differentiation and axonal elongation was induced by addition of forskolin (75 μM) into the culture medium. Within hours following forskolin treatment, more than 90% cells stopped dividing and extended long neurites. Methylglyoxal was administered at the final concentration for 20-24 h post-differentiation of the cells. For testing the effects of Podocarpic acid alone, the compound was added at a final concentration of 250 μM and incubated for the same period with or without methylglyoxal. Ethanol was used as a vehicle control. Differential Interference Contrast (DIC) imaging was performed using a Nikon Ti PFS fitted with a Cascade 512B EMCCD camera, Sutter filter wheels, and Xenon light source with constant temperature enclosure and CO_2 regulation at the stage. Neurite outgrowth was quantified by manually measuring the length of a projection from the edge of the cell body; a neurite was defined as a thin projection longer than the diameter of the associated cell body. Area of soma or cell body was measured excluding the neurite projections. Images were processed using Image Analyst MKII software (https://www.imageanalyst.net/) and quantification was done using Image J software (http://imagej.nih.gov/ij/). 75-100 cells selected randomly were considered for quantification under each experimental condition.

SUPPLEMENTAL REFERENCES

S1. Stiernagle, T. (2006). Maintenance of C. elegans. WormBook, 1-11.

S2. Onken, B., and Driscoll, M. (2010). Metformin induces a dietary restriction-like state and the oxidative stress response to extend C. elegans Healthspan via AMPK, LKB1, and SKN-1. PloS one *5*, e8758.

S3. An, J.H., and Blackwell, T.K. (2003). SKN-1 links C. elegans mesendodermal specification to a conserved oxidative stress response. Genes & development *17*, 1882-1893.

S4. Wang, J., Robida-Stubbs, S., Tullet, J.M., Rual, J.F., Vidal, M., and Blackwell, T.K. (2010). RNAi screening implicates a SKN-1-dependent transcriptional response in stress resistance and longevity deriving from translation inhibition. PLoS genetics *6*.

S5. Fensgard, O., Kassahun, H., Bombik, I., Rognes, T., Lindvall, J.M., and Nilsen, H. (2010). A two-tiered compensatory response to loss of DNA repair modulates aging and stress response pathways. Aging *2*, 133-159.

S6. Pierce-Shimomura, J.T., Chen, B.L., Mun, J.J., Ho, R., Sarkis, R., and McIntire, S.L. (2008). Genetic analysis of crawling and swimming locomotory patterns in C. elegans. Proceedings of the National Academy of Sciences of the United States of America *105*, 20982-20987.

S7. Hart, A. (2006). Behavior. WormBook.

S8. MacLean, B., Tomazela, D.M., Shulman, N., Chambers, M., Finney, G.L., Frewen, B., Kern, R., Tabb, D.L., Liebler, D.C., and MacCoss, M.J. (2010). Skyline: an open source document editor for creating and analyzing targeted proteomics experiments. Bioinformatics *26*, 966-968.

S9. Chaplen, F.W., Fahl, W.E., and Cameron, D.C. (1998). Evidence of high levels of methylglyoxal in cultured Chinese hamster ovary cells. Proceedings of the National Academy of Sciences of the United States of America *95*, 5533-5538.

S10. Henning, C., Liehr, K., Girndt, M., Ulrich, C., and Glomb, M.A. (2014). Extending the spectrum of alpha-dicarbonyl compounds in vivo. The Journal of biological chemistry *289*, 28676-28688.

S11. Rabbani, N., and Thornalley, P.J. (2014). Measurement of methylglyoxal by stable isotopic dilution analysis LC-MS/MS with corroborative prediction in physiological samples. Nature protocols *9*, 1969-1979.

S12. Thornalley, P.J., and Rabbani, N. (2014). Assay of methylglyoxal and glyoxal and control of peroxidase interference. Biochemical Society transactions *42*, 504-510.